JOURNAL OF MATERIALS SCIENCE 28 (1993) 1631–1638

Some properties of aluminium nitride powder synthesized by low-pressure chemical vapour deposition

K. ITATANI, K. SANO, F. S. HOWELL, A. KISHIOKA, M. KINOSHITA
Department of Chemistry, Faculty of Science and Technology, Sophia University, 7-1 Kioi-cho, Chiyoda-ku, Tokyo 102, Japan

Aluminium nitride (AlN) powders were synthesized by a low-pressure chemical vapour deposition, i.e. reactions of vaporized aluminium with various compositions of NH_3–N_2 gases at 1050 °C under a pressure of 0.1–1.3 kPa. The properties of the resulting powders were divided into three categories, according to the NH_3 content in the NH_3–N_2 gases: (i) $0 \leqslant NH_3 < 40\%$, (ii) $40 \leqslant NH_3 \leqslant 60\%$, and (iii) $60 < NH_3 \leqslant 100\%$. In Region (i), the unreacted aluminium adhered to the AlN crystallites to form spherical primary particles; in Region (ii), the spherical agglomerates with diameters of 0.2–0.5 μm, composed of primary particles, were present as minimum units of secondary particles; in Region (iii), the crystal growth of AlN was enhanced with increasing NH_3 contents. The primary particles formed by the reaction of aluminium vapour with NH_3–N_2 gases containing $NH_3 \geqslant 40\%$ were single crystals.

1. Introduction

Aluminium nitride (AlN) ceramics are expected to be available as substrates for semiconductors, because they have high electric resistivity, high thermal conductivity, and thermal expansion coefficients close to that of silicon [1]. AlN powder is now produced industrially by two techniques [1]: (i) the direct nitridation of aluminium powder and (ii) the carbothermal reduction of aluminium oxide (Al_2O_3).

Recent attention has been directed toward the chemical vapour deposition (CVD), i.e. the synthesis of AlN powder by the reaction of aluminium vapour with NH_3 or N_2 gas, to produce submicrometre uniform sizes of primary particles. In the CVD technique, the selection of aluminium or an aluminium compound as a vaporization source is the key to the synthesis of sinterable AlN powder. The sources reported so far are aluminium chloride ($AlCl_3$) [2–4], tri-*i*-buthylaluminium ($Al(i\text{-}Bu)_3$) [5] and aluminium [6–9]. Of these sources, aluminium has the advantage of providing high-purity AlN powder without the worry of contaminants such as halogens, hydrocarbons and carbon; however, the vaporization of aluminium requires the use of special techniques, e.g. electron-beam heating [6], arc melting [7, 8] and r.f. plasma [9], because the high boiling temperature (~2470 °C) of aluminium makes vaporization difficult.

This paper describes the synthesis of AlN powder by low-pressure CVD, i.e. the reaction of vaporized aluminium with NH_3 and/or N_2 gases at low pressures below ~1 kPa, using electric current heating to vaporize aluminium; this heating technique has the advantage of using a simpler and less expensive reaction apparatus than in the above three methods. In addition, the effects of gas compositions (NH_3/N_2) on powder properties were examined, because gas composition may affect the powder properties.

2. Experimental procedure

2.1. Reaction apparatus

The reaction apparatus for the synthesis of the AlN powder was assembled by the present authors. A schematic illustration of this apparatus is shown in Fig. 1. It was composed of (i) a mixing zone of NH_3 and N_2 gases, (ii) a reaction zone of aluminium vapour with NH_3 gas and/or N_2 gas, (iii) a collecting zone of the resulting powder, and (iv) an evacuation zone. Each zone will be explained in this section.

2.1.1. Mixing of NH_3 and N_2 gases

The mixing zone was composed of reservoirs (D, E; 3000 cm^3) of NH_3 gas (A; 99.99% pure) and N_2 gas (B; over 99.9995% pure, < 0.5 p.p.m. O_2, < 1.0 p.p.m. CO, < 1.0 p.p.m. CO_2 and < 1.0 p.p.m. CH_4), piston pump (G), and stirring mixer (F). The mixing zone was evacuated by a rotary pump (O) and an oil-diffusion pump (N); then each reservoir (D, E) was filled with NH_3 gas and N_2 gas. These gases were circulated into the mixing zone by the piston pump (G) and were mixed homogeneously by passing through the stirring mixer (F); the compositions of mixed gases were 0% NH_3–100% N_2 (pure N_2), 20% NH_3–80% N_2, 40% NH_3–60% N_2, 60% NH_3–40% N_2, 80% NH_3–20% N_2 and 100% NH_3–0% N_2 (pure NH_3).

0022–2461

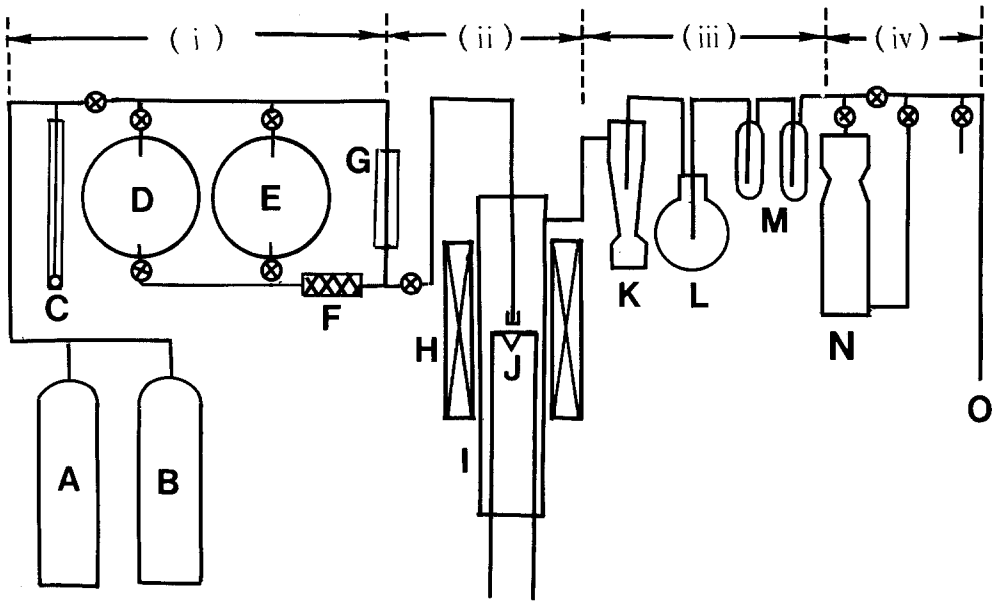

Figure 1 Schematic illustration of the reaction apparatus. A, NH_3 gas; B, N_2 gas; C, mercury manometer; D, reservoir (N_2); E, reservoir (NH_3); F, stirring mixer; G, piston pump; H, electric furnace; I, fused silica; J, BN crucible (filament: tungsten); K, cyclone; L, collector; M, trap; N, oil-diffusion pump. (i) Mixing zone of NH_3/N_2 gases, (ii) reacting zone, (iii) collecting zone, (iv) evacuation zone.

2.1.2. Reaction of aluminium with NH_3 and/or N_2

About 0.2 g commercial aluminium powder with over 99.9% purity (Kojundo Chemical Laboratories Co., Sakado, Japan) was put into a boron nitride crucible (J), which was set into the coils of the tungsten filaments coated with zirconia-based cement. The aluminium powder was vaporized at ~1800 °C, and the maximum voltage and current applied to the tungsten filament were 100 V and 35 A, respectively. The aluminium vapour reacted with NH_3 and/or N_2 to form solid materials in the fused silica tube (I, length 60 cm, i.d. 3.6 cm) which was heated by an electric furnace (H, heating region 30 cm) at 1050 °C.

2.1.3. Collecting of resulting powder

The collecting zone was composed of a cyclone (K), a cylinder-type filter (L) and traps (M). Although cyclone and filter were set in this zone, most of the solid materials were deposited on the upper walls of the fused silica tube. The traps were set to collect the unreacted aluminium vapour and NH_3 gas to prevent the pumps from corroding.

2.1.4. Evacuation

The evacuation was carried out by the rotary pump (O) and the oil-diffusion pump (N).

2.2. Evaluation of powder properties

The crystalline phases of the synthesized powders were examined using an X-ray diffractometer (XRD; Model Rad II A, Rigaku, Tokyo) with CuK_α radiation (40 kV, 25 mA); the crystalline phases were identified by checking them with JCPDS cards.

The specific surface area of the resulting powder was measured by the BET technique, using N_2 as an adsorption gas.

The crystallite size, G_{XRD}, was calculated by Scherrer's formula, using XRD

$$G_{XRD} = \frac{K\lambda}{\beta\cos\theta} \quad (1)$$

where K represents the constant (= 0.9), λ the wavelength (= 0.15405 nm) of CuK_{α_1} radiation, β the half-width of the reflection (1 0 3), and θ the Bragg angle.

The primary particle size, G_{BET} was calculated on the basis of specific surface area, assuming the primary particles to be spherical

$$G_{BET} = \frac{6}{\rho s} \quad (2)$$

where ρ represents the powder density and s the specific surface area.

The secondary particles were measured using a centrifugal sedimentation apparatus (Model CP-50, Shimadzu, Tokyo); here ethanol was used as the dispersion medium.

The particle morphology was observed using a transmission electron microscope (TEM: Model H-300, Hitachi, Tokyo) and a scanning electron microscope (SEM: Model S-430, Hitachi, Tokyo); TEM was used to observe the morphology of individual primary particles, whereas SEM was used to examine the agglomeration states of primary particles.

3. Results and discussion

3.1 Thermal reaction of aluminium vapour with NH_3–N_2 gases

The crystalline phases of powders formed by the thermal reactions of aluminium vapour with NH_3–N_2 gases were examined by XRD. Typical results are

shown in Fig. 2. The pure N_2 gas reacted with aluminium vapour to form AlN [10]; however, a large amount of aluminium [11] remained in the powder (Fig. 2a). Not only 60% NH_3–40% N_2 gas but also pure NH_3 gas reacted with aluminium vapour to form only AlN [10] (Fig. 2b and c); the intensities of AlN reflections in Fig. 2c were higher than those in Fig. 2b.

The overall trend, including the omitted XRD patterns, revealed that the reactions of NH_3–N_2 gases containing $0 \leqslant NH_3 < 40\%$ with aluminium vapour produced AlN, together with unreacted aluminium, whereas the reactions of NH_3–N_2 gases containing $40\% \leqslant NH_3 \leqslant 100\%$ with aluminium vapour produced only AlN; the intensities of AlN reflections increased with increasing NH_3 content in the NH_3–N_2 gases.

The above results suggest that the reactions of N_2 or NH_3 with aluminium vapour proceed as follows:

$$N_2 + 2Al \rightarrow 2AlN \quad (3)$$

$$NH_3 + Al \rightarrow AlN + 3/2H_2 \quad (4)$$

The following two routes have also been reported by Uda *et al.* [8]

$$NH_2 + Al \rightarrow AlN + H_2 \quad (5)$$

$$NH + Al \rightarrow AlN + 1/2H_2 \quad (6)$$

The progress of the reactions in Equations 5 and 6 requires the dissolution of NH_3 during heating

$$NH_3 \rightarrow NH_2 + 1/2H_2 \quad (7)$$

$$NH_2 \rightarrow NH + 1/2H_2 \quad (8)$$

$$NH \rightarrow 1/2H_2 + 1/2N_2 \quad (9)$$

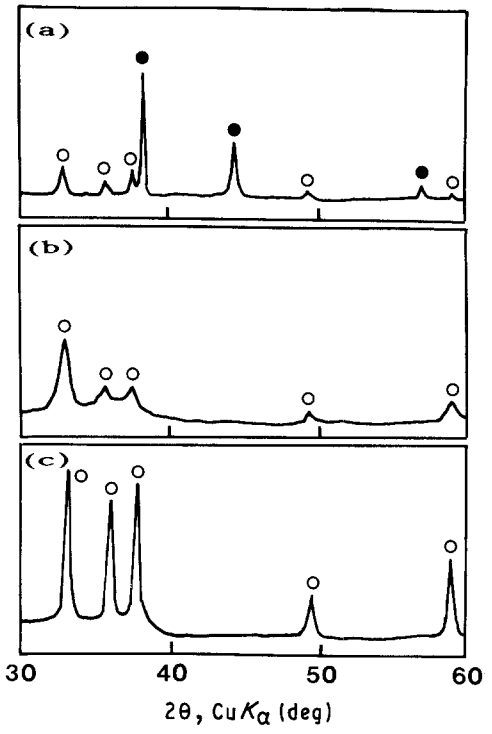

Figure 2 X-ray diffraction patterns of (a) powder formed by Al/N_2 reaction, (b) powder formed by Al/40% NH_3–60% N_2 reaction and (c) powder formed by Al/NH_3 reaction. (●) Al, (○) AlN.

Because the aluminium vapour reacts with NH_3 and/or N_2 gases at 1050 °C (1323 K), Gibb's free energies of the above reactions were obtained from the data reported by Uda *et al.* [8], who rearranged the JANAF Thermochemical Tables [12, 13]. The values corresponding to Equations 3–9 are given below.

$$\Delta G^0_{1323\,K} = -355\ kJ\,mol^{-1} \quad (3)$$

$$\Delta G^0_{1323\,K} = -270\ kJ\,mol^{-1} \quad (4)$$

$$\Delta G^0_{1323\,K} = -390\ kJ\,mol^{-1} \quad (5)$$

$$\Delta G^0_{1323\,K} = -485\ kJ\,mol^{-1} \quad (6)$$

$$\Delta G^0_{1323\,K} = +125\ kJ\,mol^{-1} \quad (7)$$

$$\Delta G^0_{1323\,K} = +95\ kJ\,mol^{-1} \quad (8)$$

$$\Delta G^0_{1323\,K} = -310\ kJ\,mol^{-1} \quad (9)$$

The data for ΔG^0_{1323K} given above indicate that the reaction of aluminium vapour with NH_3–N_2 gases may proceed via Reaction 6, because NH formed by the dissolution of NH_3 has a higher reactivity than N_2, NH_3 and NH_2.

The oxygen content of AlN powder formed by Al/40% NH_3–60% N_2 reaction was ~ 8%, according to the data measured by a high-temperature combustion technique. The presence of the oxygen in the powder may be due to the chemisorption of H_2O on the surfaces of primary particles [4]; this assumption is supported by the results of infrared spectroscopy, where a broad absorption band showing the presence of H_2O appears in the range 4000–3000 cm^{-1}. The oxygen may have been incorporated into the AlN powder during handling in air [4].

3.2. Some properties of the resulting powders

The yields of the powders formed by the thermal reactions of aluminium vapour with NH_3–N_2 gases containing $\geqslant 40\%$ NH_3 were ~ 25% theoretical. Some properties of the powders formed by Al/NH_3–

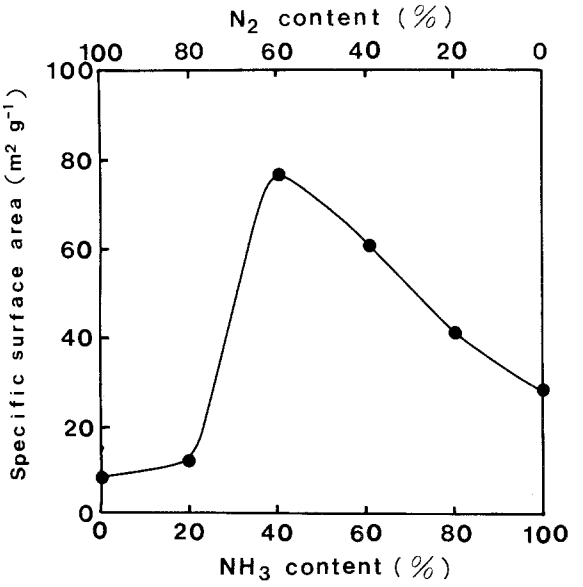

Figure 3 Changes in specific surface area of resulting powder as functions of NH_3 and N_2 compositions.

N_2 reactions were examined from the viewpoints of specific surface area (Fig. 3), particle morphologies (Figs 4 and 5), and crystallite size, primary particle size and secondary particle size (Figs 6 and 7).

The specific surface areas of the resulting powders were plotted against the compositions of NH_3–N_2 gases. Results are shown in Fig. 3. The specific surface area of the resulting powder was 8.1 m^2g^{-1} at 0% NH_3–100% N_2 gas mixture. The specific surface area increased with increasing NH_3 contents and attained a maximum (77.5 m^2g^{-1}) at 40% NH_3–60% N_2 gas mixture. A further increase in NH_3 content decreased the specific surface area down to 28.7 m^2g^{-1} at 100% NH_3–0% N_2 gas mixture.

The above behaviour can be divided into two categories, according to the NH_3 contents, i.e. $0 \leqslant NH_3 < 40\%$ and $40\% \leqslant NH_3 \leqslant 100\%$. These phenomena may be explained on the basis of the XRD data. In region $0\% \leqslant NH_3 < 40\%$, the specific surface area is enhanced by the formation of minute AlN crystals, reducing the amount of unreacted aluminium. In region $40\% \leqslant NH_3 \leqslant 100\%$, the specific surface area is reduced by the crystal growth of AlN.

The morphologies of particles were observed by TEM. Typical results are shown in Fig. 4. Here the particles observed by TEM are regarded as primary particles which are composed of one or more crystallites [14]. The results obtained are summarized below.

(a) Reaction of aluminium with N_2 (Fig. 4a). The primary particles were spherical; the diameters of these primary particles were ~ 0.2 μm. The spherical particles are regarded as assemblages of AlN and aluminium crystallites. Referring to the presence of spherical particles. Uda and Ohno [15] reported that spherical particles form when aluminium remains in the powder.

(b) Reaction of aluminium with 40% NH_3–60% N_2 (Fig. 4b). The shape of the primary particles was polyhedral with a size of ~ 0.02 μm; these primary particles were linked together to form agglomerates. The primary particle sizes are about one-tenth of those of the powder synthesized by Al/N_2 reaction (Fig. 4a); the stoichiometric reaction between aluminium and NH_3–N_2 gases seems to produce these small particles, because XRD data (Fig. 2) show that the unreacted aluminium disappears after the reaction of

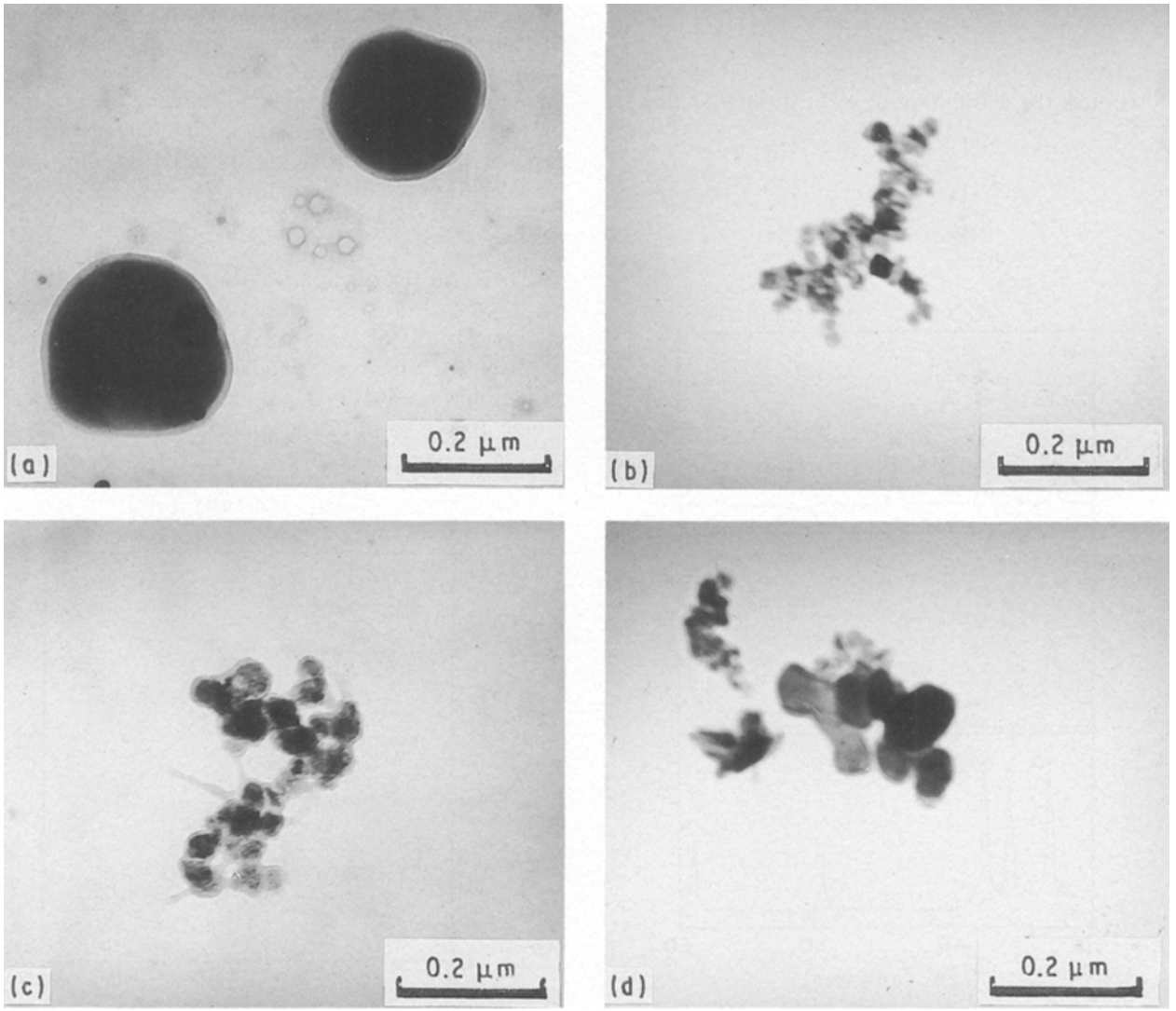

Figure 4 Transmission electron micrographs of (a) powder formed by Al/N_2 reaction, (b) powder formed by Al/40% NH_3–60% N_2 reaction, (c) powder formed by Al/80% NH_3–20% N_2 reaction, and (d) powder formed by Al/NH_3 reaction.

aluminium vapour with NH_3–N_2 gases containing 40% NH_3.

(c) Reaction of aluminium with 80% NH_3–20% N_2 (Fig. 4c). The shapes of primary particles were polyhedral and the sizes were ~ 0.05 μm. These primary particles were coagulated to form agglomerates. The primary particle sizes are about twice as large as those of the powder synthesized by Al/40% NH_3–60% N_2 reaction (Fig. 4b); thus crystal growth of AlN occurs with increasing NH_3 content.

(d) Reaction of aluminium with NH_3 (Fig. 4d). The shapes of primary particles were polyhedral and partly hexagonal; the sizes were ~ 0.1 μm. These primary particles were linked together. The linking of the primary particles indicates that the more the NH_3 content increases, the more the crystal growth of the resulting AlN is promoted. The particle shapes are close to hexagonal, which may reflect the crystal system (hexagonal) of AlN.

The agglomeration state of primary particles was examined by SEM; the secondary particle sizes were also measured quantitatively by the sedimentation technique. These data are shown in Figs. 5 and 6, respectively. The results can be summarized as follows.

(a) Reaction of aluminium with N_2. The scanning electron micrograph (Fig. 5a) showed that spherical particles with diameters of 0.2–0.5 μm were present in the powder. The histogram of the secondary particle size distribution (Fig. 6a) showed that the particle sizes were distributed over the range 0–3.2 μm; the frequency for sizes from 0.8–1.2 μm appeared to be maximum (30%). The spherical particles observed by SEM correspond to the primary particles, because their sizes are in agreement with those of primary particles shown in Fig. 4a. The secondary particle sizes are distributed over the range 0–3.2 μm, which indicates that some primary particles are dispersed individually and others are coagulated to form secondary particles.

(b) Reaction of aluminium with 40% NH_3–60% N_2. Spherical particles were present in the resulting powder (Fig. 5b); the particle diameters (0.2–0.5 μm) were roughly in agreement with those found in the case of Al/N_2 reaction (Fig. 5a). The histogram of the secondary particle size distribution (Fig. 6b) showed that

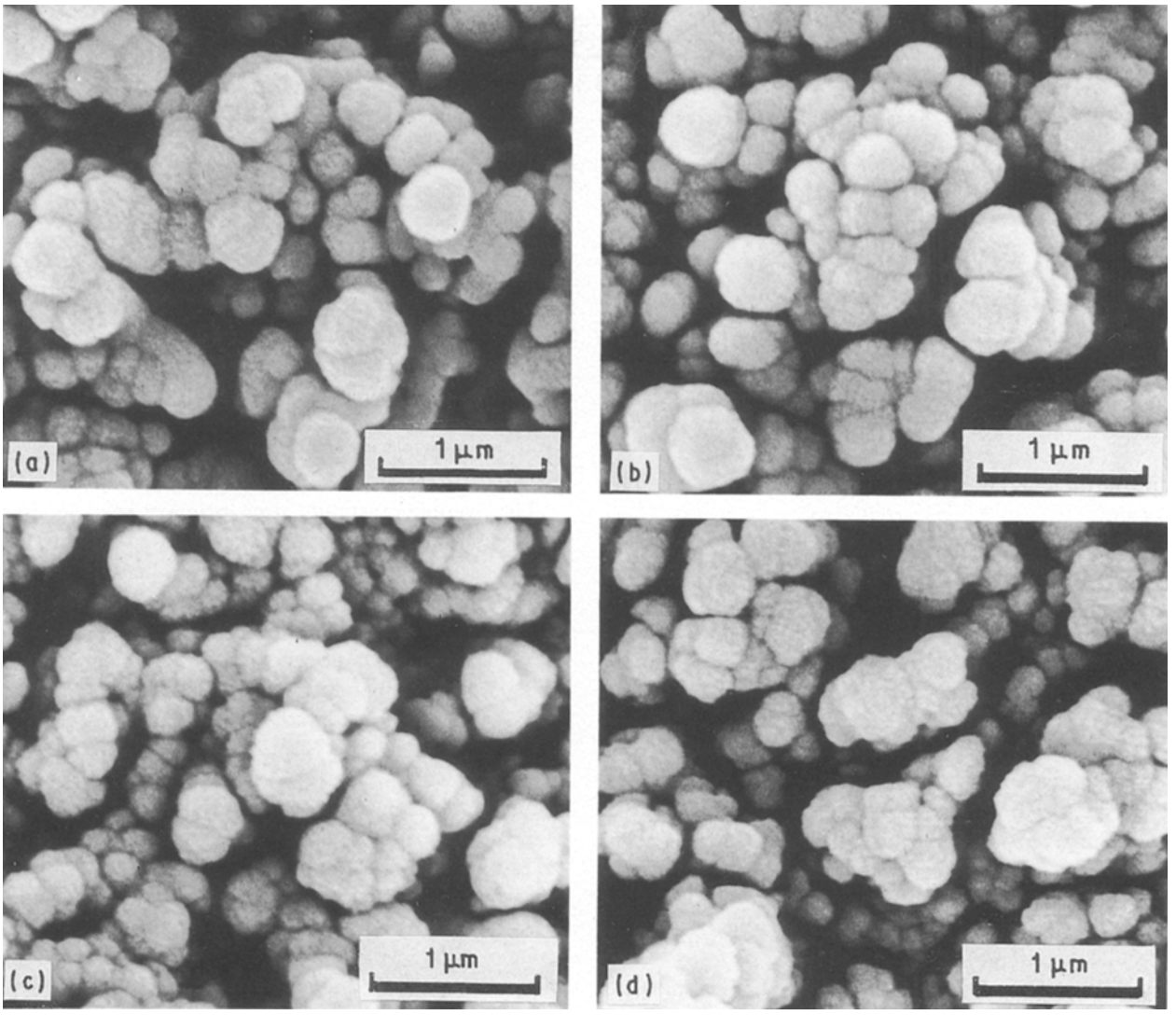

Figure 5 Scanning electron micrographs of (a) powder formed by Al/N_2 reaction, (b) powder formed by Al/40% NH_3–60% N_2 reaction, (c) powder formed by Al/80% NH_3–20% N_2 reaction, and (d) powder formed by Al/NH_3 reaction.

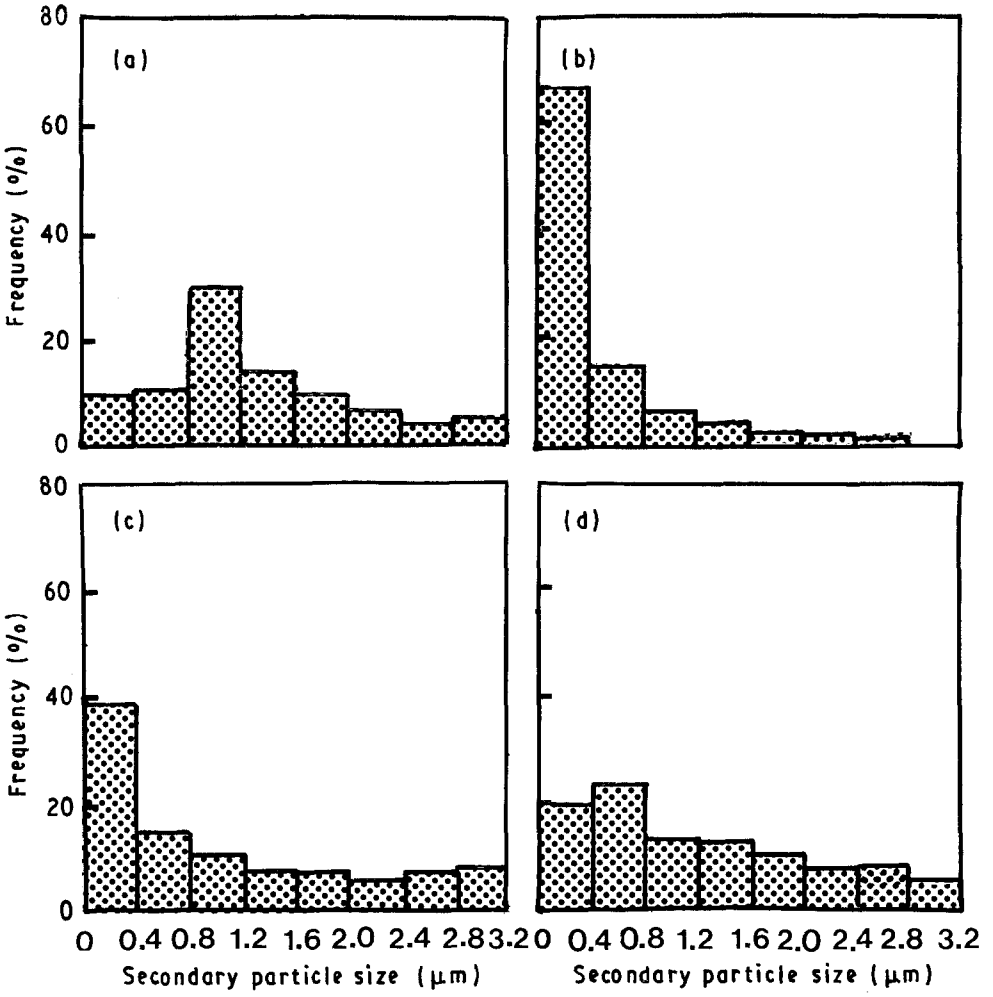

Figure 6 Histograms of secondary particle size distributions of (a) powder formed by Al/N_2 reaction, (b) powder formed by Al/40% NH_3–60% N_2 reaction, (c) powder formed by Al/80% NH_3–20% N_2 reaction, and (d) powder formed by Al/NH_3 reaction.

the maximum frequency attained 68% at sizes below 0.4 μm. The spherical particles observed by SEM correspond to the minimum units of the secondary particles. Although these spherical particles are coagulated to form larger secondary particles, they will not have strong adhesion forces, as shown in the histogram with a maximum frequency of 68% at sizes up to 0.4 μm.

(c) Reaction of aluminium with 80% NH_3–20% N_2. Spherical particles were present in the powder (Fig. 5c); the particle diameters (0.2–0.5 μm) were almost the same as those reported in (a) and (b). The histogram of the secondary particle size distribution (Fig. 6c) revealed that the particle sizes had maximum frequency (39%) at sizes below 0.4 μm; however, this frequency was lower than that (68%) reported in (b). As already explained in (b), the spherical particles observed by SEM correspond to minimum units of the secondary particles. Because the frequency at sizes below 0.4 μm is lower than that reported for 40% NH_3–60% N_2, the agglomeration of these spherical particles seems to be promoted with increasing NH_3 content.

(d) Reaction of aluminium with NH_3. The particle sizes (0.2–0.5 μm) observed by SEM (Fig. 5d) were almost the same as those reported in (a)–(c). The histogram of the secondary particle size distribution (Fig. 6d) showed that the secondary particle sizes were distributed over the range 0–3.2 μm. The histogram of the secondary particle size distribution demonstrates that the spherical particles agglomerate with one another with increasing NH_3 content; the agglomeration of spherical particles may proceed by the crystal growth of AlN.

The average crystallite sizes, primary particle sizes and secondary particle sizes were plotted against the compositions of NH_3–N_2 gases. The results are shown in Fig. 7. The crystallite sizes of AlN were almost constant ($\sim$ 0.03 μm) in the range 0% $\leqslant NH_3 < 60\%$; however, the crystallite size increased to $\sim$ 0.05 μm on increasing the NH_3 content up to 100%. On the other hand, the primary particle size was $\sim$ 0.2 μm at 0% NH_3–100% N_2 (pure N_2); it decreased with increasing NH_3 content and became almost the same as the crystallite size for the 40% NH_3–60% N_2 gas mixture; a further increase in NH_3 content brought about primary particle growth. The secondary particle size decreased with increasing NH_3 contents and attained a minimum ($\sim$ 0.6 μm) value at 40% NH_3–60% N_2 gas mixture; however, it increased on increasing the NH_3 content up to 100%.

The information obtained from the above results is summarized as follows: (i) The primary particle sizes become much larger than crystallite sizes in the

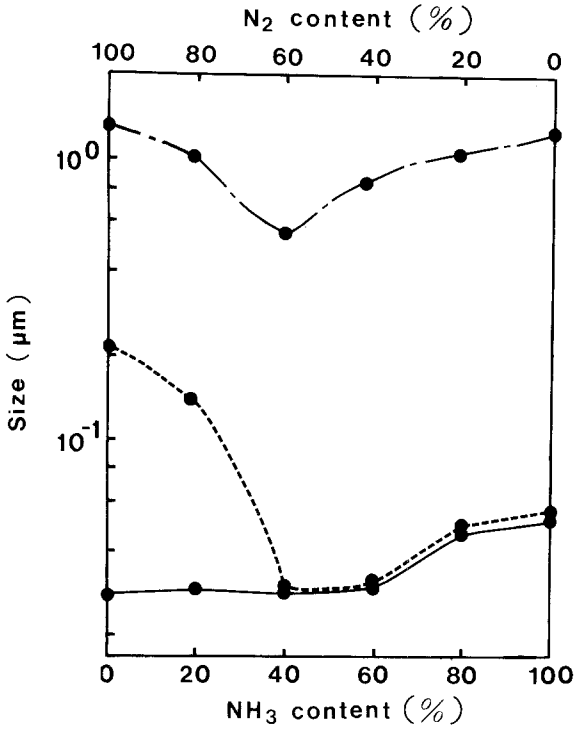

Figure 7 Changes in (——) crystallite (AlN) size, (– – –) primary particle size, and (—— – ——) secondary particle size as functions of NH_3 and N_2 compositions.

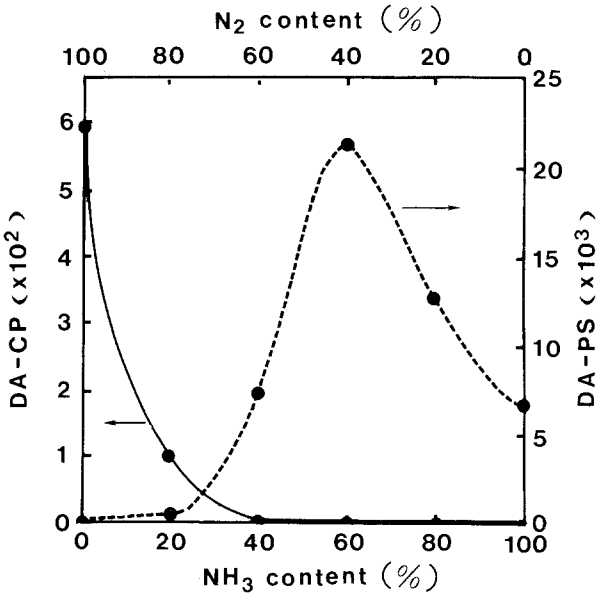

Figure 8 Changes in degrees of agglomerations of (——) crystallites per primary particle (DA–CP) and (– – –) primary particles per secondary particle (DA–PS) as functions of NH_3 and N_2 compositions.

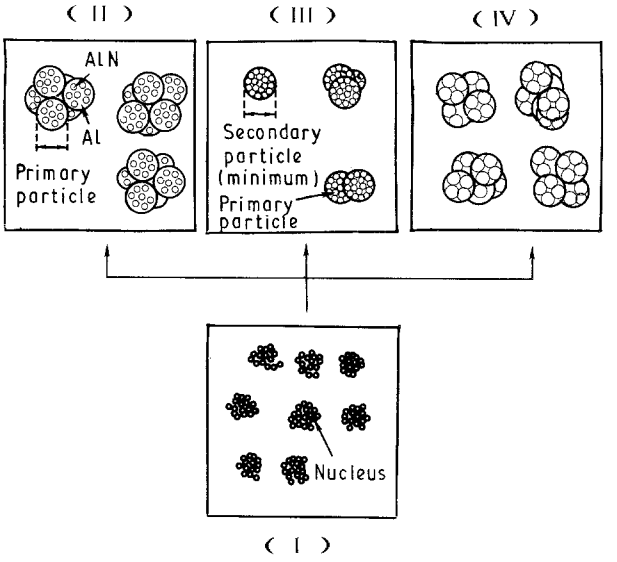

Figure 9 Schematic illustrations of agglomeration state of resulting powders synthesized by low-pressure CVD. (I) Nucleation of AlN and/or unreacted aluminium, (II) formation of spherical primary particles containing AlN and/or unreacted aluminium ($0\% \leqslant NH_3 < 40\%$), (III) formation of the spherical agglomerate as a minimum unit of secondary particles; the coagulation of these spherical agglomerates produces the larger secondary particles ($40\% \leqslant NH_3 \leqslant 60\%$), (IV) crystal growth of AlN within spherical agglomerates ($60\% < NH_3 \leqslant 100\%$).

range $0\% \leqslant NH_3 < 40\%$, (ii) the primary particle size is almost in agreement with the crystallite size in the range $40\% \leqslant NH_3 \leqslant 100\%$, and (iii) the secondary particle size becomes a minimum at 40% NH_3–60% N_2 gas mixture. Phenomenon (i) may be attributed to the adhesion of AlN crystallites, where the unreacted aluminium may act as a bonding agent. Phenomenon (ii) suggests the primary particles to be single crystals, whereas phenomenon (iii) indicates the presence of well-dispersed agglomerates corresponding to the minimum units of secondary particles.

As the data shown in Figs 2–7 indicate, the resulting powders are composed of various "units" of agglomerates. Therefore, we calculated the degrees of agglomeration of crystallites per primary particle (DA–CP) and of primary particles per secondary particle (DA–PS) [16, 17]. The results are shown in Fig. 8. The DA–CP value was ~ 600 at 0% NH_3–100% N_2 gas mixture; it decreased suddenly with increasing NH_3 content and became ~ 1 in the $40\% \leqslant NH_3 \leqslant 100\%$ range. On the other hand, the DA–PS value increased with increasing NH_3 content and attained a maximum ($\sim 22 \times 10^3$) at 60% NH_3–40% N_2 gas mixture. A further increase in NH_3 content decreased the DA–PS value to $\sim 7 \times 10^3$.

The DA–CP values are much larger than unity in the $0\% \leqslant NH_3 < 40\%$ range, which suggests that the unreacted aluminium may act as a bonding agent of AlN crystallites. These DA–CP values become nearly unity in the $40\% \leqslant NH_3 \leqslant 100\%$ range; the primary particles prove to be single crystals. On the other hand, the DA–PS value attains a maximum at 60% NH_3–40% N_2 gas mixture; this fact suggests that the small primary particles deposited from the gas phase cause some agglomeration due to the electrostatic and van der Waals forces [18].

The overall results shown in Figs 2–8 allow us to conclude that the powder properties can be divided into three categories, according to the NH_3 contents: (i) $0\% \leqslant NH_3 < 40\%$, (ii) $40\% \leqslant NH_3 \leqslant 60\%$, and (iii) $60\% < NH_3 \leqslant 100\%$. Some schematic illustrations of these powder properties are shown in Fig. 9.

The thermal reaction of aluminium vapour with NH_3 and/or N_2 forms nuclei of AlN and/or aluminium (unreacted materials) (Fig. 9, Region I); these nuclei are linked together to show agglomeration. In Region II, $0\% \leqslant NH_3 < 40\%$, the spherical primary particles are formed by assemblages of AlN crystallites; the unreacted aluminium acts as a bonding agent. In Region III, $40\% \leqslant NH_3 \leqslant 60\%$, the spherical agglomerates formed by the coagulation of primary particles are present as minimum units of secondary particles; the more the NH_3 content increases, the more the agglomeration of the resulting AlN particles proceeds. In Region IV $60\% < NH_3 \leqslant 100\%$, the primary particle size is enhanced by the crystal growth of AlN.

4. Conclusions

Aluminium nitride (AlN) powders were synthesized by a low-pressure chemical vapour deposition; AlN powder was formed by the reaction of aluminium vapour with ammonia (NH_3) gas and/or nitrogen (N_2) gas at 1050 °C under a pressure of 0.1–1.3 kPa. The results obtained are as follows.

1. The crystalline phases of powders formed by the thermal reaction of aluminium vapour with NH_3–N_2 gases containing $< 40\%$ NH_3 were AlN and aluminium, whereas those formed by the reaction of aluminium vapour with NH_3–N_2 gases containing $\geqslant 40\%$ NH_3 were only AlN.

2. The powder properties could be divided into three categories according to the NH_3 content in the NH_3–N_2 gases: (i) $0\% \leqslant NH_3 < 40\%$, (ii) $40\% \leqslant NH_3 \leqslant 60\%$, and (iii) $60\% < NH_3 \leqslant 100\%$. In Region (i), $0\% \leqslant NH_3 < 40\%$, the unreacted aluminium adhered to the AlN crystallites to form spherical primary particles. In Region (ii), $40\% \leqslant NH_3 \leqslant 60\%$, the spherical agglomerates formed by the coagulation of primary particles were present as minimum units of secondary particles; the more the NH_3 content increases, the more the coagulation of these agglomerates proceeds. In Region (iii), $60\% < NH_3 \leqslant 100\%$, the crystal growth of AlN was enhanced with increasing NH_3 content. The primary particles formed by the reaction of aluminium vapour with NH_3–N_2 gases containing $\geqslant 40\%$ NH_3 were single crystals.

Acknowledgements

The authors thank Mr Shigeru Ando for advice on assembling the reaction apparatus, and Ube Chemical Industries Ltd, for providing the hot-pressed BN body.

References

1. N. HASHIMOTO, Y. SAWADA, T. BANDO, H. YODEN and S. DEKI, *J. Amer. Ceram. Soc.* **74** (1991) 1282.
2. I. KIMURA, N. HOTTA, H. NUKUI, N. SAITO and S. YASUKAWA, *Seramikkusu Ronbunshi* **96** (1988) 206.
3. I. KIMURA, N. HOTTA, H. NUKUI, N. SAITO and S. YASUKAWA, *J. Mater. Sci.* **24** (1989) 4076.
4. R. RIEDEL and K.-U. GAUDL, *J. Amer. Ceram. Soc.* **74** (1991) 1331.
5. K. TSUCHIDA, Y. TAKESHITA, A. YAMANE and A. KATO, *Yogyo-Kyokai-Shi* **95** (1987) 1198.
6. S. IWAMA, K. HAYAKAWA and T. AKIZUMI, *J. Crystal Growth* **56** (1982) 265.
7. G. P. VISSOKOV and L. B. BRAKALOV, *J. Mater. Sci.* **18** (1983) 2011.
8. M. UDA, S. OHNO and H. OKUYAMA, *Yogyo-Kyokai-Shi* **95** (1987) 86.
9. M. YOKOTA, S. YAGYU, K. MAJIMA and H. NAGAI, *J. Jpn. Soc. Powder Powder Metall.* **38** (1991) 382.
10. Powder diffraction file Card no. 25-1133 (JCPDS-International Center for Diffraction Data, Pennsylvania, USA).
11. Powder diffraction file Card no. 4-787 (JCPDS-International Center for Diffraction Data, Pennsylvania, USA).
12. D. R. STULL and H. PROPHET, "JANAF Thermochemical Tables", 2nd Edn, NSRD-NBS 37 (1971).
13. M. W. CHASE Jr, J. L. CURNUTT, J. R. DOWNEY Jr, R. A. McDONALD, A. N. SYVERUD and E. A. VALENZUELA, "JANAF Thermochemical Table", 1982 Supplement, *J. Phys. Chem. Ref. Data* **11** (1982) 695.
14. K. ITATANI, M. NOMURA, A. KISHIOKA and M. KINOSHITA, *J. Mater. Sci.* **21** (1986) 1429.
15. M. UDA and S. OHNO, *Nippon Kagaku Kaishi* **1984** (1984) 862.
16. K. ITATANI, K. KOIZUMI, F. S. HOWELL, A. KISHIOKA and M. KINOSHITA, *J. Mater. Sci.* **23** (1988) 3405.
17. *Idem, ibid.* **24** (1989) 2603.
18. H. RUMPF and H. SCHUBERT, in "Ceramic Processing before Firing", edited by G. Y. Onoda and L. L. Hench (Wiley, New York, 1978) p. 61.

Received 22 November 1991
and accepted 2 September 1992